Multiple visible emissions by means of up-conversion process in a microstructured tellurite glass optical fiber

Multiple visible emissions by means of up-conversion process in a microstructured tellurite glass optical fiber

Nadia G. Boetti,[1,*] Joris Lousteau,[1] Davide Negro,[1] Emanuele Mura,[1] Gerardo Scarpignato,[1] Silvio Abrate,[2] and Daniel Milanese[1]

[1]PhotonLab, Dipartimento di Scienza Applicata e Tecnologia, Politecnico di Torino, Corso Duca degli Abruzzi 24 10129 – Torino, Italy

[2]PhotonLab, Istituto Superiore Mario Boella, Via P.C. Boggio, 61, 10138 – Torino, Italy

**nadia.boetti@polito.it*

Abstract: We present a microstructured fiber whose 9 µm diameter core consists in three concentric rings made of three active glasses having different rare earth oxide dopants, Yb^{3+}/Er^{3+}, Yb^{3+}/Tm^{3+} and Yb^{3+}/Pr^{3+}, respectively. Morphological and optical characterization of the optical fiber are presented. The photoluminescence spectrum is investigated for different pumping conditions using a commercial 980 nm laser diode. Tuning of the RGB (or white light) emission is demonstrated not only by adjusting the pump power but also by using an optical iris as spatial filter which, thanks to the microstructured core, also acts as a spectral filter.

OCIS codes: (060.4005) Microstructured fibers; (060.2280) Fiber design and fabrication; (230.6080) Sources.

References and Links

1. M. C. B. Jaffe, S. M. Jaffe, and A. R. Conner, "New lighting for the design of high quality biomedical devices," Proc. SPIE **7170**, 71700M, 71700M-9 (2009).
2. X. Zhu and N. Peyghambarian, "High-power ZBLAN glass fiber lasers: review and prospect," Adv. Optoelectron. **2010**, 501956 (2010).
3. J. S. Wang, E. M. Vogel, and E. Snitzer, "Tellurite glass: a new candidate for fiber devices," Opt. Mater. **3**(3), 187–203 (1994).
4. D. H. Cho, Y. G. Choi, and K. H. Kim, "Improvement of $^4I_{11/2}$ -> $^4I_{13/2}$ transition rate and thermal stabilities in Er^{3+}-doped TeO_2-B_2O_3(GeO_2)-ZnO-K_2O glasses," ETRI J. **23**(4), 151–157 (2001).
5. P. V. dos Santos, M. V. D. Vermelho, E. A. Gouveia, M. T. de Araujo, A. S. Gouveia-Neto, F. C. Cassanjes, S. J. L. Ribeiro, and Y. Messaddeq, "Infrared-to-visible up-conversion in Pr^{3+}/Yb^{3+} and Er^{3+}/Yb^{3+} codoped tellurite glasses," J. Alloy. Comp. **344**(1-2), 304–307 (2002).
6. Y. Yang, W. Zhang, S. Guo, and Z. Yang, "Compositional dependence of up-conversion emission and optical transition in Yb^{3+}-Ho^{3+} codoped tellurite-phosphate glasses," Proc. SPIE **7749**, 77490T (2010).
7. J. Zhang, S. Dai, G. Wang, L. Zhang, H. Sun, and L. Hu, "Investigation on upconversion luminescence in Er^{3+}/Yb^{3+} codoped tellurite glasses and fibers," Phys. Lett. A **345**(4-6), 409–414 (2005).
8. S. Q. Xu, H. P. Ma, D. W. Fang, Z. X. Zhang, and Z. H. Jiang, "Upconversion luminescence and mechanism in Yb^{3+}- sensitized Tm^{3+}- doped oxyhalide tellurite glasses," J. Lumin. **117**(2), 135–140 (2006).
9. H. T. Bookey, J. Lousteau, A. Jha, N. Gayraud, R. R. Thomson, N. D. Psaila, H. Li, W. N. MacPherson, J. S. Barton, and A. K. Kar, "Multiple rare earth emissions in a multicore tellurite fiber with a single pump wavelength," Opt. Express **15**(26), 17554–17561 (2007).
10. F. Auzel, "Upconversion and anti-Stokes processes with f and d ions in solids," Chem. Rev. **104**(1), 139–174 (2004).
11. J. C. Wright, "Up-conversion and excited state energy transfer in rare-earth doped materials," Top. Appl. Phys. **15**, 239–295 (1976).
12. R. Scheps, "Upconversion laser processes," Prog. Quantum Electron. **20**(4), 271–358 (1996).
13. Y. Dwivedi, A. Rai, and S. B. Rai, "Intense white upconversion emission in Pr/Er/Yb codoped tellurite glass," J. Appl. Phys. **104**(4), 043509 (2008).
14. S. X. Dai, J. H. Yang, S. Q. Xu, N. L. Dai, L. Wen, L. L. Hu, and Z. H. Jiang, "Multi-rare-earth ions codoped tellurite glasses for potential dual wavelength fibre-optic amplifiers," Chin. Phys. Lett. **20**(1), 130–132 (2003).
15. N. K. Giri, D. K. Rai, and S. B. Rai, "White light upconversion emissions from Tm^{3+} Ho^{3+} Yb^{3+} codoped tellurite and germanate glasses on excitation with 798 nm radiation," J. Appl. Phys. **104**(11), 113107 (2008).

#160147 - $15.00 USD Received 20 Dec 2011; revised 8 Feb 2012; accepted 15 Feb 2012; published 21 Feb 2012

16. D. L. Yang, H. Gong, E. Y. B. Pun, X. Zhao, and H. Lin, "Rare-earth ions doped heavy metal germanium tellurite glasses for fiber lighting in minimally invasive surgery," Opt. Express **18**(18), 18997–19008 (2010).
17. Z. Yang and Z. Jiang, "Frequency upconversion emissions in layered lead–germanate–tellurite glasses for three-color display," J. Non-Cryst. Solids **351**(30-32), 2576–2580 (2005).
18. J. Lousteau, N. G. Boetti, D. Negro, E. Mura, G. Scarpignato, M. Raimondo, S. Abrate, and D. Milanese, "Rare-earth doped tellurite glass optical fiber for visible light sources," Transparent Optical Networks (ICTON), 2011 13th International Conference 1–4, 26–30 June (2011).
19. X. Feng, F. Poletti, A. Camerlingo, F. Parmigiani, P. Horak, P. Petropoulos, W. H. Loh, and D. J. Richardson, "Dispersion-shifted all-solid high index-contrast microstructured optical fiber for nonlinear applications at 1.55 microm," Opt. Express **17**(22), 20249–20255 (2009).
20. H. R. Müller, J. Kirchhof, V. Reichel, and S. Unger, "Fibers for high-power lasers and amplifiers," C. R. Phys. **7**(2), 154–162 (2006).
21. J. Lousteau, N. G. Boetti, A. Chiasera, M. Ferrari, S. Abrate, G. Scarciglia, A. Venturello, and D. Milanese, "Er^{3+} and Ce^{3+} co-doped tellurite optical fiber for lasers and amplifiers in the near infrared wavelength region: fabrication, optical characterization and prospects," IEEE Photon. J. **4**(1), 194–204 (2012).
22. A. S. Gouveia-Neto, E. B. Da Costa, L. A. Bueno, and S. J. L. Ribeiro, "Red, green, and blue upconversion luminescence in ytterbium-sensitized praseodymium-doped lead-cadmium-germanate glass," Opt. Mater. **26**, 271–274 (2004).
23. C. B. de Araújo, L. S. Menezes, G. S. Maciel, L. H. Acioli, A. S. L. Gomes, Y. Messaddeq, A. Florez, and M. A. Aegerter, "Infrared-to-visible CW frequency upconversion in Er^{3+}-doped fluoroindate glasses," Appl. Phys. Lett. **68**(5), 602 (1996).
24. D. Milanese, H. Gebavi, J. Lousteau, M. Ferraris, A. Schülzgen, L. Li, N. Peyghambarian, S. Taccheo, and F. Auzel, "Tm^{3+} and Yb^{3+} co-doped tellurite glasses for short cavity optical fiber lasers: fabrication and optical characterization," J. Non-Cryst. Solids **356**, 2378–2383 (2010).
25. N. G. Boetti, J. Lousteau, A. Chiasera, M. Ferrari, E. Mura, G. C. Scarpignato, S. Abrate, and D. Milanese, "Thermal stability and spectroscopic properties of erbium-doped niobic-tungsten–tellurite glasses for laser and amplifier devices," J. Lumin. **132**(5), 1265–1269 (2012).
26. D. Manzani, Y. Ledemi, I. Skripachev, Y. Messaddeq, S. J. L. Ribeiro, R. E. P. de Oliveira, and C. J. S. de Matos, "Yb^{3+}, Tm^{3+} and Ho^{3+} triply-doped tellurite core-cladding optical fiber for white light generation," Opt. Mater. Express **1**(8), 1515–1526 (2011).

1. Introduction

Numerous application fields such as optical sensing, biological analysis, biomedical diagnostics, Red Blue Green (RGB) display require the use of radiation sources either broadband or single frequency operating at visible wavelengths [1].

Nowadays, several well mastered technologies allow to produce such sources, see for instance Table 1 in [1]. However, each of these techniques present one or several disadvantages that do not allow to achieve the range of performances required by the applications foreseen.

A possible alternative to engineer visible light sources, either in the form of laser or broadband source, relies on up-conversion mechanism that can occur in rare-earth (RE) ion elements when pumped with an infrared laser source. This physical process has been exploited since the 90s to produce visible light lasers from fluoride glasses using red or near-IR pump laser sources (see for example Table 3 in [2]). However, fluoride glasses suffer from poor chemical durability and require stringent manufacturing process to avoid crystallization. Nonetheless, other glass materials and pumping schemes are available.

Amongst the possible glassy materials able to host rare-earth ions, tellurite glasses possess properties well adapted to ignite up-conversion mechanisms. Those are: ability to accept large concentrations of ions without clustering, high refractive index and more interestingly a low phonon energy [3]. The latter property is of particular importance for what concerns up-conversion mechanism. Like for fluoride glasses, the low phonon energy of tellurite glasses allow for long lifetime of metastable states through which the electrons transit to the upper levels that lead to visible emission. For instance the typical lifetime of the $4I_{11/2}$ level of Er^{3+} in tellurite glass is 200 μs, while in silica glass its value is less than 10 μs [4].

Furthermore, using trivalent ytterbium Yb^{3+} as a sensitizer enhances the up-conversion efficiency [5]. Through its high absorption cross-section and simple energy structure, the Yb^{3+} ion provides an efficient energy transfer path towards the acceptor ion (A) with a limited

#160147 - $15.00 USD Received 20 Dec 2011; revised 8 Feb 2012; accepted 15 Feb 2012; published 21 Feb 2012

backward energy transfer from the latter [2]. Moreover the presence of Yb^{3+} ions allow the use of bright commercial infrared single mode 980nm laser diodes for pumping.

In recent years many studies have reported on the spectroscopic analysis of RE ion pairs such as Yb^{3+}/Ho^{3+}, Yb^{3+}/Pr^{3+}, Yb^{3+}/Tm^{3+} or Yb^{3+}/Er^{3+} in tellurite bulk glass [5–9]. The up-conversion mechanisms for these ions pairs have been extensively described in literature, e.g [5–12].

With the aim to engineer multiple wavelengths, broadband or white light sources, several studies [13–16] have also discussed the investigation of tellurite glass bulk samples triply doped with the rare-earth ions mentioned above. Indeed the possibility for one glass to host several Yb^{3+}/A pairs appears appealing. However, as discussed in [17], the presence of several RE ions in the same glass matrix leads to detrimental energy transfer phenomena. These interactions quench the visible emissions of each acceptor ion and reduce the efficiency of the overall up-conversion process.

To overcome this issue, Yang et al. [17] suggested to separate spatially emitting ions by a layered structure where each layer embeds one Yb^{3+}/A pair. Also beneficial for up-conversion process is the tight optical confinement provided by waveguide structures. However, up to now only few works have reported on the generation of visible emission within a tellurite glass optical fiber [7,9].

Combining both layered and waveguide structures, we report on the fabrication and the characterization of a broadband visible light source in the form of a microstructured RE doped tellurite glass optical fiber. The core of this fiber consists of three concentric rings doped with different Yb^{3+}/A pairs that can be simultaneously pumped with a single commercial laser diode operating at 980 nm.

2. Experimental procedure

2.1 Glass Composition and fabrication

Compositions of the four glasses fabricated in this work are reported in Table 1. The three compositions named for short TZN1, TZN2 and TZN3 were designed to be part of the fiber core surrounded by a cladding made of the passive glass composition TZN4.

TZN1, TZN2 and TZN3 were doped with the three RE-ions pairs Yb^{3+}/Tm^{3+}, Yb^{3+}/Pr^{3+} and Yb^{3+}/Er^{3+}, respectively. These three ion pairs were selected on the basis of their reported suitability for up-conversion process in tellurite glass [5,8]. In particular, the combined visible emission spectra of Tm^{3+}, Pr^{3+} and Er^{3+} cover a large bandwidth of the visible spectrum with several emission peaks at the red, green and blue wavelengths.

After mixing, the batched chemicals were transferred into a Pt crucible for melting. The melting procedure was carried out inside a glove box under dried air atmosphere with a water level lower than 7 ppm. The onset melting temperature was 750 °C and the duration of the process 3 h. The furnace temperature was lowered down to 720 °C for 1 hour prior to casting. The melt was then cast in a brass mould preheated at Tg −10 °C and annealed at the same temperature for 1h.

In order to engineer a suitable refractive index profile distribution into the fiber, the amount of tellurium dioxide was progressively reduced from TZN1 to TZN4 and in replacement sodium oxide quantity was increased. Table 1 shows RE ions concentration in weight percentage added to the glass host and the refractive index of each glass host composition at a wavelength of 633 nm.

Details on glass fabrication and characterization can be found in [18].

2.2 Fiber design and fabrication

To exploit the individual up-conversion emission observed in Yb^{3+}/Er^{3+}, Yb^{3+}/Pr^{3+} and Yb^{3+}/Tm^{3+} co-doped tellurite bulk glass samples, the fiber was designed to have a core

#160147 - $15.00 USD Received 20 Dec 2011; revised 8 Feb 2012; accepted 15 Feb 2012; published 21 Feb 2012

consisting of two concentric rings made from glasses TZN2 and TZN3 that surround a central circular area made of glass TZN1.

The three glass compositions were designed to provide a decreasing refractive index profile when going from the center of the core towards the cladding zone. A schematic diagram of the fiber cross section is reported in Fig. 1.

Table 1. Composition and refractive index of the tellurite glasses used to manufacture the optical fiber presented in this paper.

Glass label	Composition (mol%)	RE ions added (wt%)		n at 633 nm ± 0.001
TZN1	79TeO_2:15ZnO:6 Na_2O	Yb_2O_3	1	2.067
		Tm_2O_3	0.1	
TZN2	78 TeO_2:15ZnO:7Na_2O	Yb_2O_3	1	2.056
		Pr_2O_3	0.3	
TZN3	77TeO_2:15ZnO:8Na_2O	Yb_2O_3	1	2.044
		Er_2O_3	0.15	
TZN4 cladding	75TeO_2:15ZnO:10Na_2O	-	-	2.022

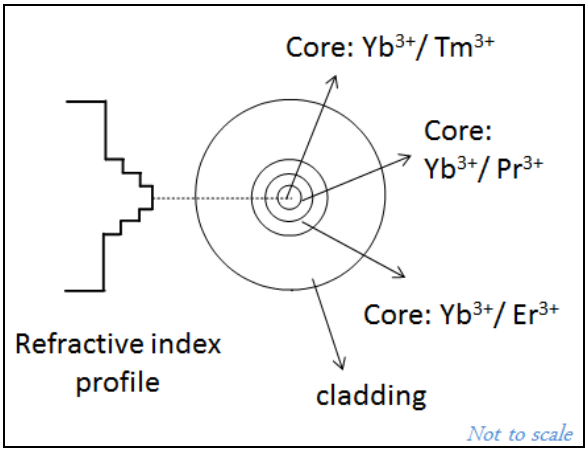

Fig. 1. Simplified schematic diagram of fiber cross section

The choice of a core made of concentric layers allows to incorporate several types of emitting ions while limiting the interaction of pairs with one another. Such interaction could quench the visible emission through non radiative energy transfer processes. Despite the refractive index structure, some interaction between acceptor ions by field overlap and evanescent field is still to be expected. Similar concentric structures have been already developed to tailor the dispersion properties of passive optical fibers for telecom [19]. An analogy in terms of field propagation of the pump can also be made with double cladding fiber geometries used for high power fiber lasers [20]. Actually, the fiber was developed (see details below) so that the dimension of the triple layer structure fiber, 9 µm in diameter, would match closely the dimension of the pumping fiber core, 6 µm in diameter. Adding that the index contrast between TZN4 and TZN3 provided a numerical aperture (NA) of 0.3 to ensure multimode operation at 980 nm; the fiber was thus designed so that an efficient and homogeneous pumping along short fiber length could be achieved.

In terms of emission field interaction, the fiber was designed so that the numerical apertures of 0.3 between adjacent layers limits the penetration of evanescent field from internal layers into the adjacent external cladding layer. In a similar fashion to what occurs in double cladding fiber, the emission field arising from external layers can propagate through

#160147 - $15.00 USD Received 20 Dec 2011; revised 8 Feb 2012; accepted 15 Feb 2012; published 21 Feb 2012

the internal layers of higher refractive index. However, this interaction between rare-earth ions is limited to radiative processes which could be minimized or possibly exploited through adequate fiber designs optimized via propagation field modeling technique.

The fiber was manufactured by preform drawing using a drawing tower developed in-house. The fiber preform fabrication required the manufacture of one rod of glass TZN1 obtained by melt quenching and three tubes of glasses TZN2, TZN3 and TZN4 shaped by rotational casting at 3000 rpm. Although tellurite glass shows a good resistance against crystallization upon reheating, the preform fabrication process was drawn up to minimize the number of reheating steps for each glass composition.

The drawing tower furnace consists in a graphite ring heated by an induction operating at 248 kHz and delivering 170 W to reach drawing temperature (SAET, Torino). The preform was fed into the furnace and drawn into fiber at a speed of 2.5 m/min under a tension of 70 mN at a temperature of 370°C. About 200 m of uncoated pristine fiber were drawn without showing any sign of crystallization.

2.3 Property measurements

Fiber photoluminescence spectra in the visible range were recorded by exciting a 5 cm long fiber sample with a single mode 978 nm fiber pigtailed laser diode coupled by butt-coupling. The output emission was measured by a fiber spectrometer (Avantes, AvaSpec-2048x14). The resolution of the spectrometer was 2 nm and its sensitivity was tuned by changing the integration time in order to get the highest spectrum dynamics while avoiding saturation. The spectrometer comes with a predefined wavelength calibration stored in the on-board EEPROM, so the measured spectra are automatically corrected from the instruments spectral response.

To avoid disturbance from the residual pump during measurements, a wideband hot-mirror (Thorlabs FM01) at 980 nm was placed at the end of the fiber. The photoluminescence spectrum of the fiber output was measured for the following pump powers, 6 mW, 15 mW, 70 mW, 125 mW.

Fiber emission intensity in the visible range was measured using an UV enhanced silicon photodetector (Newport 818-UV).

All measurements were performed at room temperature.

The concentric configuration of the tellurite glass fiber presented here has an additional advantage. Not only the individual emissions from the three core regions can be easily combined along their common optical axis but more interestingly they can be also spatially separated through a simple optical setup like the one shown in Fig. 2. The optical bench consists of a near field imaging setup with an iris adequately positioned further down the optical path. The iris acts then not only as a spatial filter but also as a simple optical wavelength filter that permits for selecting one particular zone of the spectrum or for tuning the RGB emission.

#160147 - $15.00 USD Received 20 Dec 2011; revised 8 Feb 2012; accepted 15 Feb 2012; published 21 Feb 2012

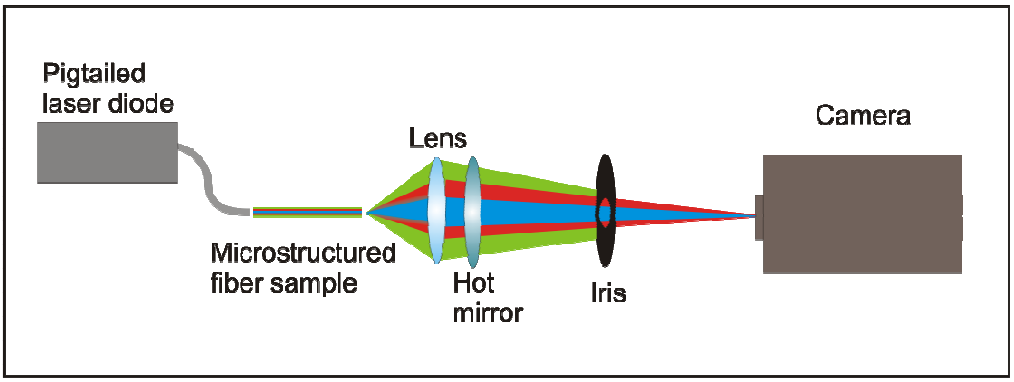

Fig. 2. Optical setup used to tune the RGB emission by spatial filtering. The colored beam illustrates the multi-wavelength emission arising from the core structured in concentric layers

3. Results and discussion

The morphology of the fiber and, in particular, of the microstructured core was investigated. Figure 3 shows an optical micrograph of the fiber cross-section (a) and a scanning electron micrograph image taken in back-scattering mode (b). In this latter image the dimension of the different concentric layers of glass TZN1, TZN2 and TZN3 are reported. It can be seen that the core is made in large part of TZN3 doped with Er^{3+}. This is due to an unwanted collapse of the TZN2 tube during the manufacture of the preform.

In spite of the small central layer dimension of 1.6 µm in diameter, due to the large NA of 0.3 between adjacent layers and the short emission wavelengths, none of the layers was found to operate in the single mode regime at the photoemission wavelengths.

Due to the lack of suitable sources operating at wavelengths outside the rare earth multiple absorption peaks, it was not possible to carry out standard cut-back measurements. Nonetheless optical losses are assumed to be of the same order of magnitude (~1 dB/m) to that of passive tellurite glass fibers manufactured in our laboratory using the same fabrication procedure [21].

The fiber photoluminescence spectrum in the visible range is reported in Fig. 4, where emission peaks are labeled with the corresponding RE ions level transitions. The spectrum was arbitrarily normalized on the intensity of the most intense emission peak of Er^{3+} ion $^4S_{3/2}\rightarrow{}^4I_{15/2}$. Actually, as one can observe on the fiber emission spectrum shown in Fig. 4, the intensity of the peak centered at 546 nm (Er^{3+}: $^4S_{3/2}\rightarrow{}^4I_{15/2}$) appears to be higher than other emission peaks from other RE ions. It should also be highlighted that during the measurements an intense green light arising from the fiber could be observed to the naked eye. This observation suggests not only that green emission from Er^{3+} exceed other emissions in terms of absolute power, but also that the confinement of spontaneous emission is relatively low.

#160147 - $15.00 USD Received 20 Dec 2011; revised 8 Feb 2012; accepted 15 Feb 2012; published 21 Feb 2012

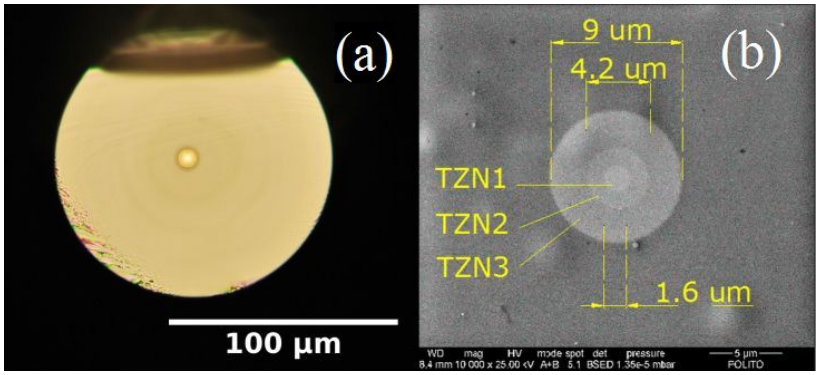

Fig. 3. Optical microscope image of the tellurite glass fiber cross-section (a) and scanning electron micrograph image taken in back-scattering mode (b)

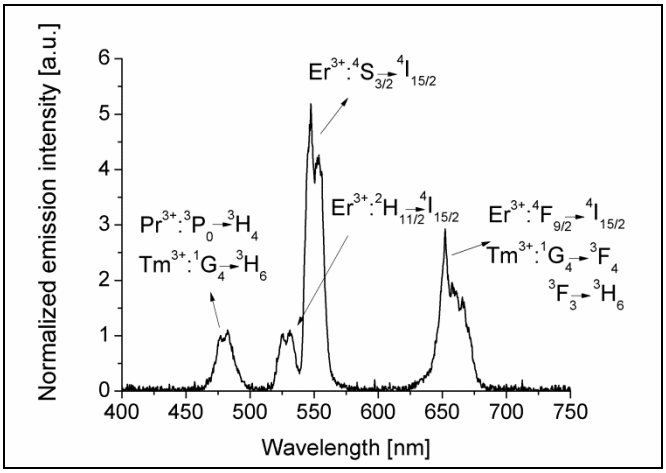

Fig. 4. Fiber photoluminescence upon 978 nm excitation

Although the emission from all three Tm^{3+}, Er^{3+} and Pr^{3+} ions could be detected, the magnitude of the emission from Pr^{3+} ions collected out of the fiber is considerably lower than the others, as also observed in bulk glass fluorescence measurements. Actually unlike reported by [22], this observation suggests that the 980 nm is not well adapted for pumping the pair Yb^{3+}/Pr^{3+} and generate visible up-conversion. In fact 980 nm pump photons will be absorbed by Yb^{3+} ions in the ground state, then these latter will transfer their energy to Pr^{3+} ions promoting them to the $^1G_4$ intermediate level by energy transfer (ET). At this point 980 nm pump photons will not possess enough energy to promote efficiently Pr^{3+} ions to the $^3P_0$ level by excited state absorption (ESA). As suggested by numerous reports in literature a more viable pumping scheme of the Yb^{3+}/Pr^{3+} pair relies on the use of a pump source operating at 850 nm [2].

During fluorescence measurements, it was also noticed that the relative intensity of the peaks one to another can be altered by adjusting the input pump power, as reported in Fig. 5. Similar effect has already been reported by [23] and is of interest for tunable RGB applications. The general trend is that the magnitude of long wavelength peaks decrease at the expense of short wavelengths peaks, while increasing the input pump power. This effect can be explained as follows.

#160147 - $15.00 USD Received 20 Dec 2011; revised 8 Feb 2012; accepted 15 Feb 2012; published 21 Feb 2012

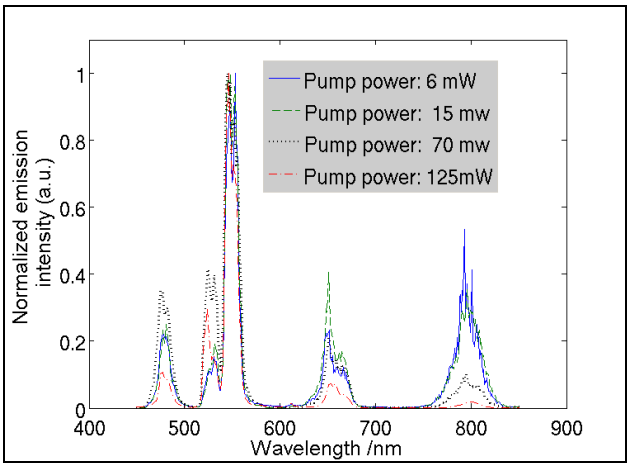

Fig. 5. Fibre photoluminescence for different input pump power

In Tm^{3+} ion, the peak emission centered at 650 nm arises from both the $^1G_4 \rightarrow {}^3F_4$ transition and the $^3F_{2,3} \rightarrow {}^3H_6$ transition, while the peak emission centered around 800 nm arise from the transition from $^3H_4 \rightarrow {}^3H_6$ $^3H_6$ (see for details the schematic RE ions energy-level diagram reported in Fig. 6). Although population of the $^1G_4$ level requires a 3 photons process [8], population of the $^3F_{2,3}$ and $^3H_4$ levels can occur through excited state absorption from the $^3F_4$ level. Not only, this two-step process requires solely 2 photons but also the "metastable or transitional" level $^3F_4$ possesses a relatively long lifetime in tellurite glass, typically of the order of 2 ms, which favors the ESA process [24]. In other words, even for low incoming photon density level, $^3F_{2,3}$ and $^3H_4$ levels get populated while population of the more energetic level $^1G_4$ remains limited. As the incoming photon density increases population of the $^1G_4$ level increases at the expense of the direct population of the $^3F_{2,3}$ and $^3H_4$ level by ESA from the $^3H_4$ levels.

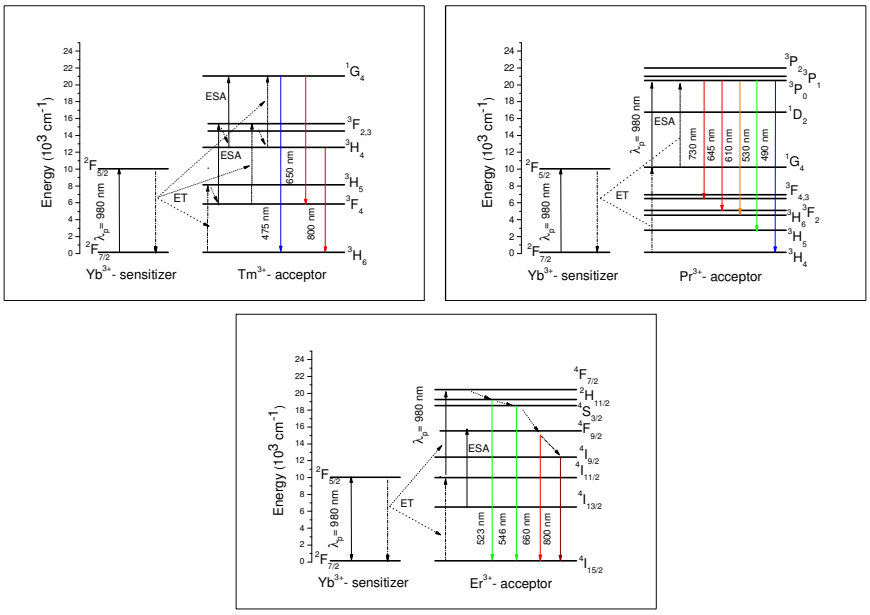

Fig. 6. Schematic energy-level diagram for the Yb^{3+}/Tm^{3+}, Yb^{3+}/Pr^{3+} and Yb^{3+}/Er^{3+} doped tellurite glasses

#160147 - $15.00 USD Received 20 Dec 2011; revised 8 Feb 2012; accepted 15 Feb 2012; published 21 Feb 2012

A similar discussion can be held regarding the Er^{3+} ion, where population of the $^4F_{9/2}$ and $^4I_{9/2}$ levels, leading respectively to peak emissions centered at 650 nm and 800 nm, can occur either via the $^2H_{11/2}$ followed by a multiphonon decay or directly via ESA from level $^4I_{13/2}$, which in tellurite glass presents a lifetime typically of the order of 3 ms [25]. The former case occurs for high photon density and leads to an intense green emission centered around 546 nm corresponding to the $^2H_{11/2} \rightarrow {}^4I_{15/2}$transition, while the latter case occurs at low incoming photon density.

The relative intensity of the peaks one another can also be altered by tuning the fiber length. Like in the case of a decreasing pump power, an increase of the fiber length will lead to an increase of magnitude of long wavelength peaks at the expense of short wavelengths peaks, due to reduced photon density towards the fiber end extremity.

The pump power absorbed by 5 cm of the microstructured fiber was measured to be 10 mW for 100 mW launched power giving rise to a visible fiber emission power of about 10 µW. Although such an output power value remains low in terms of efficiency (only 0.1%), it is nonetheless about 6 times higher than recent results [26] obtained for a tellurite glass fiber 10 cm long whose core was doped with $Yb^{3+}/Ho^{3+}/Tm^{3+}$ and that had a surface area about 10 times larger. This preliminary comparison suggests a more efficient up-conversion emission process taking place in the concentric structured fiber presented here in spite of the poor up-conversion emission efficiency of Pr^{3+}.

To assess waveguiding within the fiber and analyze the spectral and spatial distributions of the output field, the near field of the end face of the fiber was imaged on a video camera. Two sections of fiber were analyzed, one 10 cm long and the other 5 cm long. Launched pumping power was 100 mW.

A wideband hot-mirror (Thorlabs FM01) was placed on the beam path to filter out the residual 980 nm pumping radiation. The resulting near field image is shown in Fig. 7a) in which one can observe the structure of the fiber through the spectral pattern of its output field. Although the emission ring from Pr^{3+} is distinguishable, its intensity appears far lower with respect to the emission arising from the Er^{3+} and Tm^{3+}. In the central core area the red emission from Tm^{3+} ($^3F_{2,3} \rightarrow {}^3H_6$) transition can be clearly distinguished. The red emission could be observed to the naked eye along the end extremity of the fiber where the blue emission from Tm^{3+} ($^1G_4 \rightarrow {}^3H_6$) was lower due to the decreasing pump intensity and re-absorption. Figure 7b) shows the output length for a 5 cm long section of fiber where the red emission from Tm^{3+} was filtered using a dichroic cyan filter (Thorlabs FD1C) to reveal the blue of emission from Tm^{3+} ($^1G_4 \rightarrow {}^3H_6$).

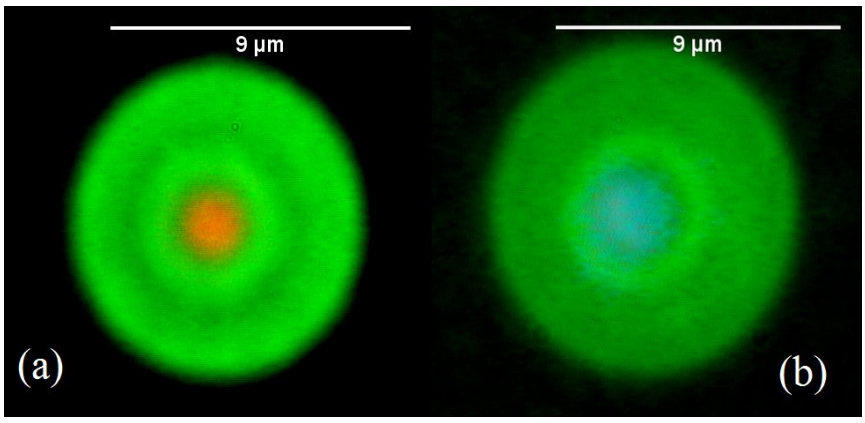

Fig. 7. Near field images of the microstructured fiber upon 978 nm excitation, without filtering (a) and with a subtractive dichroic cyan filter (b)

#160147 - $15.00 USD Received 20 Dec 2011; revised 8 Feb 2012; accepted 15 Feb 2012; published 21 Feb 2012

As already mentioned above, one could tune to some extent the output emission of the fiber by adjusting the pump power. However, one disadvantage of this approach is a non-negligible residual pump power which is detrimental for some applications. Moreover the power density at a specific wavelength would also be altered which is not a desired feature either. Instead, using an iris in a similar setup to the one shown in Fig. 2 allows one to tune the emission without requiring to the use of high pump power and without modifying the power density of the desired wavelengths. This is illustrated in Fig. 8 which shows photoluminescence spectra acquired for two distinct apertures of the iris. For the small aperture position, the reduction of the green emission from Er^{3+} is clearly distinguishable, although the emission peaks remains yet the preponderant one across the whole spectrum. This simple tuning approach illustrated one of the beneficial features of the concentrically layered tellurite glass fiber presented here.

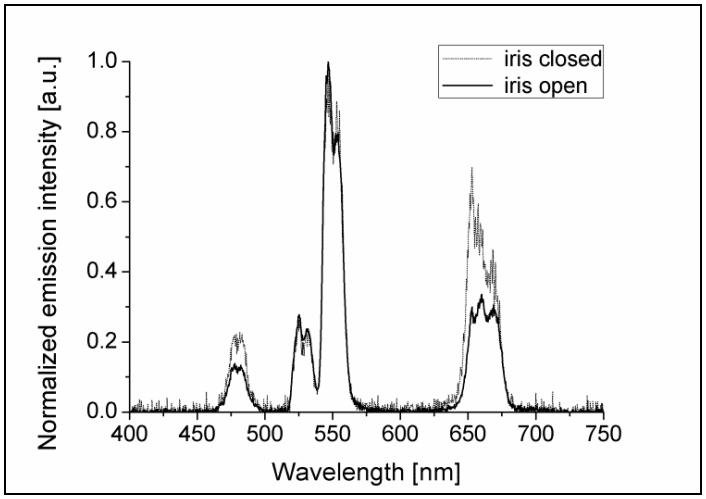

Fig. 8. Effect of spatial filtering on fibre photoluminescence upon 978 nm excitation

4. Conclusions

The optical fiber structure presented allows for exploiting individual emission from different rare-earth ions. The structured core permits to overcome potential non radiative processes and complex energy transfer between ions that would take place in a non-structured core. At the same time, emissions from all ions are guided and exit the fiber along the same optical propagation axis. This feature presents the advantage of simplifying the optical setup intended to use the emitted beam. For instance this feature makes possible the use of a simple iris as wavelength filter to tune the RGB emission.

With the aim to improve the output emission from the fiber in terms of efficiency and absolute power, further work will be carried out to optimize ions concentration level, core geometry dimensions and refractive index profile. Addition of other rare earth elements will also be considered to engineer a broadband source covering the whole visible spectrum.

Moreover addition of other RE ions should also be considered to engineer a broadband source covering the whole visible spectrum.

Acknowledgments

The authors want to thank Mauro Raimondo, DISMIC, Politecnico di Torino, for performing electron microscopy measurement on the fiber. The authors acknowledge the support of Regione Piemonte through the Converging Technologies “Hipernano” research project.

#160147 - $15.00 USD Received 20 Dec 2011; revised 8 Feb 2012; accepted 15 Feb 2012; published 21 Feb 2012